

Determining Higgs couplings with a model-independent analysis of $h \rightarrow \gamma\gamma$

Aleksandr Azatov, Roberto Contino, Daniele Del Re,
Jamison Galloway, Marco Grassi, Shahram Rahatlou*

*Dipartimento di Fisica, Università di Roma “La Sapienza”
and INFN Sezione di Roma, I-00185 Rome, Italy*

Abstract

Discovering a Higgs boson at the LHC will address a major outstanding issue in particle physics but will also raise many new questions. A concerted effort to determine the couplings of this new state to other Standard Model fields will be of critical importance. Precise knowledge of these couplings can serve as a powerful probe of new physics, and will be needed in attempts to accommodate such a new boson within specific models. In this paper, we present a method for constraining these couplings in a model-independent way, focusing primarily on an exclusive analysis of the $\gamma\gamma$ final state. We demonstrate the discriminating power of fully exclusive analyses, and discuss ways in which information can be shared between experimentalists and theorists in order to facilitate collaboration in the task of establishing the true origins of any new physics discovered at the LHC.

*email: aleksandr.azatov@roma1.infn.it, roberto.contino@roma1.infn.it, daniele.delre@roma1.infn.it,
jamison.galloway@roma1.infn.it, marco.grassi@cern.ch, shahram.rahatlou@roma1.infn.it

1 Introduction

The Higgs boson of the Standard Model (SM) is a special particle in many ways. Its exchange is required to regulate the energy behavior of the scattering amplitudes involving longitudinal vector bosons, hence ensuring the perturbative unitarity of the theory in the ultraviolet. If discovered, it would be the first example of an elementary scalar field, a new form of matter in addition to fermions and the spin-1 carriers of gauge forces. It would also imply the existence of fundamental forces (its self-interaction and the Yukawa interactions to fermions) not of gauge type. All these properties, in fact, are strictly related to the possibility for the theory to remain weakly coupled up to extremely large energies, possibly of the order of the Planck scale. This too, by itself, would be a profoundly new phenomenon in Nature: physics at the fundamental level would be described by the same mathematical theory over ~ 15 orders of magnitude in energy without any new dynamics appearing at intermediate scales. To realize this paradigm, the couplings of the Higgs boson must be finely tuned to specific values which depend uniquely on its mass. Any deviation from these values would either imply the existence of additional Higgs bosons that take part in the perturbative unitarization of the scattering amplitudes, like in the case of Supersymmetry, or signal the existence of a new energy threshold at which the theory becomes strongly coupled. In this second case the Higgs boson would emerge as a composite state of a new fundamental force [1], possibly of gauge type.

A precise measurement of the Higgs couplings will give the unique opportunity to test the SM paradigm and get information on the dynamics behind electroweak symmetry breaking (EWSB). Although the experimental searches have been so far conducted and, to a large extent, optimized in the framework of specific models (*e.g.* the Standard Model or the Minimal Supersymmetric Standard Model), the best strategy to investigate the nature of the Higgs boson and to report the experimental results is by adopting a model-independent bottom-up approach. The most general description is based on the formalism of chiral Lagrangians, supplemented by a few minimal assumptions motivated by the experimental information at our disposal. The chiral Lagrangian introduced in Ref. [2] and extended by Ref. [3] (for earlier related work see [4]) fully characterizes the interactions of a light Higgs-like scalar under the following conditions:

- new physics states, if present, are heavy and their effect at low-energy can be encoded by local operators in the chiral Lagrangian
- the EWSB dynamics possesses an (at least approximate) custodial symmetry
- there are no flavor-changing neutral currents mediated at tree-level by the Higgs.

The first assumption implies in particular that there are no new particles to which the Higgs boson can decay. It can be easily relaxed by including in the Lagrangian any new light state that should be discovered. The request of a custodial symmetry is strongly motivated by the absence of corrections to the ρ parameter measured at LEP and implies that the couplings of the Higgs to the W and the Z must be equal. Under these hypotheses, the interactions of a single Higgs-like scalar are characterized in terms of a set of parameters which describe the couplings to the SM fermions and the electroweak gauge bosons plus new contact interactions to a pair gluons or photons (as for example generated by loops of heavy scalar or fermionic top partners). Such a parameter space includes the SM as a specific point, and is sufficiently generic to describe scenarios where the Higgs-like scalar is not part of an $SU(2)_L$ doublet or is not even related to EWSB, as in the case of a light dilaton [5].²

In this paper we demonstrate how exclusive as opposed to inclusive analyses are much more powerful in determining the Higgs couplings in a model-independent approach. We will do so by focusing on the $h \rightarrow \gamma\gamma$ channel, which is the most sensible in the case of a light Higgs boson. We will restrict, for simplicity, to the case in which single Higgs interactions can be parametrized in terms of only two independent parameters: the coupling to two gauge bosons, $a = g_{hVV}/g_{hVV}^{SM}$, and the coupling to two fermions $c = g_{h\psi\psi}/g_{h\psi\psi}^{SM}$. New contact interactions mediated by heavy new physics will be assumed to be small and to have a negligible impact on the Higgs phenomenology. In this simplified framework we make a first attempt to estimate the precision that the LHC can reach on a and c with 2012 data. Our results should be compared to previous studies on the measurement of the Higgs couplings,

²By restricting to the case where the Higgs scalar is part of an $SU(2)_L$ doublet, so that the electroweak symmetry is linearly realized at high energies, the low-energy Lagrangian can be expanded in the usual series of operators with increasing dimension. In the case of a strongly-interacting light Higgs this formulation coincides with the SILH Lagrangian of Ref. [6].

which include Refs. [7–13] and the more recent Refs. [14,3,15–18]. Our exercise also illustrates how the experimental results can and should be reported in a model-independent fashion.

2 Exclusive Analysis of the $h \rightarrow \gamma\gamma$ channel

The sensitivity of the search for the Higgs boson is enhanced when events are divided into categories with different signal-to-background ratios. This division is also helpful to discriminate among different Higgs production mechanisms. In this analysis we exploit this categorization to improve the constraints in the (a, c) plane compared to an inclusive analysis. We use the $h \rightarrow \gamma\gamma$ decay since it is the most sensitive channel for a low mass Higgs, and choose $m_h = 120 \text{ GeV}$ as benchmark value for our analysis. We adopt this value mostly because efficiencies and event yields are quite often reported for this choice of m_h in the experimental papers.

We start from the CMS analyses described in Refs. [19,20]. Three variables are used to divide events based on the kinematic properties of the $\gamma\gamma$ final state and the quality of the photon reconstruction. The first variable is the transverse momentum of the $\gamma\gamma$ system, $p_T(\gamma\gamma)$, which identifies kinematic regions with smaller background contamination. It also enhances the sensitivity to vector boson fusion (VBF) and associated production (VH) mechanisms, which typically produce a Higgs boson with larger $p_T(\gamma\gamma)$ compared to those produced through gluon-gluon fusion (GGF). The second variable, called R_9 , is related to the shape of the energy deposited by the photon candidates in the electromagnetic calorimeter and helps to separate events with converted photons. Finally, the third variable is the minimum pseudorapidity η of the two photons. Eight inclusive categories are defined according to the following criteria: $p_T(\gamma\gamma) > 40 \text{ GeV}$ and $p_T(\gamma\gamma) < 40 \text{ GeV}$; large and small R_9 ; and whether both photons are in the central (barrel) region ($|\eta| < 1.44$) or at least one photon is in the endcap region ($|\eta| > 1.44$). Two additional *exclusive* categories are defined based on the presence of extra jets and leptons in the event, in order to increase the sensitivity to different production mechanisms. The first exclusive category (jj) includes events with two extra high- p_T jets in the forward region in addition to the photon candidates, and is thus enriched with Higgs bosons produced via VBF [19]. The selection requires the leading (subleading) jet to have a minimum transverse momentum of 30 GeV (20 GeV).

The two selected jets need to be separated in pseudorapidity ($|\Delta\eta_{jj}| > 3.5$), and to have a large invariant mass ($m_{jj} > 350 \text{ GeV}$). There is also the additional requirement that the difference between the average pseudorapidity of the two jets and the pseudorapidity of the diphoton system (*i.e.* the Higgs boson) has to be less than 2.5. The second exclusive category ($1l$) includes events with at least one extra lepton and is, therefore, more sensitive to Higgs candidates produced via associated production with a W/Z boson, which decays leptonically [20]. The lepton is required to be isolated and to have a transverse momentum larger than 20 GeV and a pseudorapidity which satisfies $|\eta_l| < 2.4$.

We use the signal efficiencies and backgrounds estimates reported by CMS in [19] for the eight inclusive and jj categories, and in [20] for the $1l$ category. However, the analysis proposed in this paper requires the knowledge of the signal efficiencies and the expected backgrounds in each category relative to individual production mechanisms. This information is not available in the referenced CMS analyses and, therefore, has been estimated at the generator level and extrapolated from the published results.

Di-photon events are generated with MADGRAPH [21] interfaced to PYTHIA 8.130 [22] and are used to estimate the fraction of background with $p_T(\gamma\gamma)$ above and below 40 GeV. This is done separately in each of the four categories defined by R_9 and the photon pseudorapidity. We assume this fraction to be the same also for the reducible background with at least one fake photon. This is a reasonable approximation since the reducible background is about 30% of the total. For the exclusive categories, we use the background reported in Ref. [19] for the jj class and Ref. [20] for the leptonic one. The final number of background events is obtained by performing a simple cut on $m(\gamma\gamma)$ around the Higgs mass (120 GeV), consistent with the expected CMS mass resolution, which corresponds to a $\pm 3 \text{ GeV}$ window for barrel-barrel photon categories and for the exclusive jj and leptonic categories, and a $\pm 6 \text{ GeV}$ window for photon categories with at least a photon in the endcap. The background is thus obtained by integrating the number of events estimated from data in these windows.

Since we want to scan the (a, c) plane, signal efficiencies for each category and for each of the different Higgs production mechanisms are needed. We use Montecarlo generators to determine these efficiencies. For gluon-gluon fusion and VBF we use POWHEG at next-to-leading order (NLO) [23,24], while for VH we use PYTHIA at leading order (LO). The sum of the contributions from the different production mechanisms are then scaled to give the

	$p_T(\gamma\gamma) < 40 \text{ GeV}$						$p_T(\gamma\gamma) > 40 \text{ GeV}$			
	$1l$	jj	$R_9^>$ BAR	$R_9^<$ BAR	$R_9^>$ END	$R_9^<$ END	$R_9^>$ BAR	$R_9^<$ BAR	$R_9^>$ END	$R_9^<$ END
GGF	0	0.14	3.23	3.40	1.20	1.44	1.55	1.64	0.58	0.69
VBF	0	0.44	0.067	0.071	0.026	0.031	0.17	0.18	0.066	0.079
VH	0.089	0.0035	0.059	0.063	0.028	0.033	0.17	0.18	0.081	0.097
background	0.25	2.88	85.4	126	134	188	36.4	53.7	57.7	80.3

Table 1: Number of events (per fb^{-1}) in each of the 10 categories of the exclusive analysis for the signal in the SM (for each Higgs production mode) and total background.

total number of Higgs events in the 4 photon categories and in the jj category as reported in [19] and in the leptonic category as reported in [20]. We assume that the efficiency of the $m(\gamma\gamma)$ cut described above is approximately 100% on the signal.

We derive our results for three different analyses:

- one with 4 categories based on R_9 and photon pseudorapidity variables, which makes no use of the $p_T(\gamma\gamma)$ spectrum, as in [25];
- one with 8 categories based on R_9 , photon pseudorapidity and $p_T(\gamma\gamma)$ variables to help discriminating between different production mechanisms, thanks to the harder $p_T(\text{Higgs})$ in VBF and VH mechanisms compared to gluon-gluon fusion;
- one with 8 inclusive plus two exclusive (jj and $1l$) categories, to fully exploit the physics potential.

A summary of the number of background and SM signal events expected per fb^{-1} is reported in Tab. 1 and Tab. 2 for the last two analyses. In the case of the 4-category analysis, the number of events in each of the R_9 and η classes is obtained from Tab. 2 by summing together the corresponding high and low $p_T(\gamma\gamma)$ events. Starting from the number of signal events predicted in the SM for each production mode, the number of events for arbitrary couplings a , c is easily obtained by rescaling the Higgs production cross sections and partial decay rates, as detailed in the Appendix. For each category i , given the number of signal ($n_s^i(a, c)$),

	$p_T(\gamma\gamma) < 40 \text{ GeV}$				$p_T(\gamma\gamma) > 40 \text{ GeV}$			
	$R_9^>$	$R_9^<$	$R_9^>$	$R_9^<$	$R_9^>$	$R_9^<$	$R_9^>$	$R_9^<$
	BAR	BAR	END	END	BAR	BAR	END	END
GGF	3.21	3.41	1.19	1.43	1.61	1.71	0.60	0.72
VBF	0.091	0.096	0.031	0.036	0.31	0.33	0.10	0.13
VH	0.067	0.070	0.030	0.036	0.20	0.21	0.089	0.11
background	85.8	126	135	189	36.6	53.9	58.0	80.6

Table 2: Number of events (per fb^{-1}) in each of the 8 categories of the inclusive analysis for the signal in the SM (for each Higgs production mode) and total background.

background (n_b^i) and observed events (n_{obs}^i), we construct a 2D posterior probability

$$p(a, c | n_{obs}^i) = p(n_{obs}^i | n_s^i(a, c) + n_b^i) \times \pi(a, c) \quad (2.1)$$

following the Bayesian approach.³ The total probability is then obtained as the product of the single probabilities. The likelihood function $p(n_{obs}^i | n_s^i + n_b^i)$ is modeled by a Poisson distribution, and we take a flat prior $\pi(a, c)$ on the square $-3 \leq a, c \leq +3$ (vanishing outside) as done in Ref. [3]. The effect of systematic uncertainties on the signal is taken into account by letting the fraction of signal events in each category and from each production mode fluctuate. We do so by varying all the fractions with a single nuisance parameter θ_s , so that $n_s^i \rightarrow n_s^i(1 + \theta_s)$, except for the GGF fraction in the jj category which is varied with a different parameter θ_s^{GGFjj} . The total probability is then marginalized over θ_s and θ_s^{GGFjj} , which are taken to be distributed with a truncated Gaussian with zero mean and standard deviation equal to respectively $\Delta\theta_s = 0.15$ and $\Delta\theta_s^{GGFjj} = 0.70$. This corresponds to treating the systematic errors on the signal as 100% correlated in all categories and production modes, which is a reasonable approximation considering that the largest uncertainty comes from the theoretical prediction of the Higgs production cross sections, except for the GGF events in the jj category, whose largest uncertainty originates from the efficiency of the kinematic cuts applied [19]. We neglect all systematic uncertainties on the background.

To check that all assumptions, efficiency estimates and statistical analysis are reasonable

³See for example Ref. [26] for a primer.

and robust, we derived the expected limits on the signal strength modifier considered by CMS and ATLAS, $\mu = \sigma \times BR / (\sigma \times BR)_{SM}$, in two different scenarios: in the SM hypothesis, where the limit is extracted with 4 categories to mimic the CMS analysis of [25], and in the Fermiophobic (FP) scenario, where the limit is extracted with 8+2 categories to mimic the CMS analysis of [20]. To do so we set $a = c = \sqrt{\mu}$ and $n_{obs} = n_b$ in our likelihoods, and use a flat prior on μ for $\mu > 0$ (zero otherwise) as adopted by ATLAS and CMS [27]. For a 120 GeV Higgs we find the following 95% expected limits: $\mu^{95\%} = 1.4$ for the SM case, to be compared with 1.6 reported by CMS; $\mu^{95\%} = 0.36$ for the FP case, to be compared with 0.30 reported by CMS. Both estimates are in reasonable agreement with the official value, considering the approximations done in our method. The looser limit in the FP case is probably due to the use of two $p_T(\gamma\gamma)$ categories instead of the full 2D fit approach ($m(\gamma\gamma)$ vs $p_T(\gamma\gamma)$) performed in [20].

3 Results

We now present the results of our analysis of the $\gamma\gamma$ channel for a Higgs mass of 120 GeV. As discussed in more details in the following, at the qualitative level our results apply reasonably well to the range of Higgs masses $m_h = 120 - 130$ GeV, while at the quantitative level differences can become important for $m_h \gtrsim 125$ GeV.

We start with a discussion of the expected 95% exclusion limits in the (a, c) plane, which are shown in Fig. 1 for a center-of-mass energy $\sqrt{s} = 7$ TeV and an integrated luminosity $L = 5 \text{ fb}^{-1}$, approximately the amount of luminosity accumulated individually by ATLAS and CMS in 2011. One can see that the fully-exclusive analysis with 10 categories (purple solid curve) is much more powerful in the $c \sim 0$ region compared to the inclusive analysis with 4 categories (dotted red curve), *e.g.* the one performed by CMS in Ref. [25]. For $c \rightarrow 0$ the Higgs couplings to fermions vanish and the total production cross section, which for large values of $|c|$ is strongly dominated by gluon fusion, receives its main contribution from VBF and W/Z associated production. An enhanced sensitivity to these production modes, as obtained by including the two exclusive event classes, can thus lead to much stronger constraints. An appreciable, though milder improvement on the limit is also obtained in the

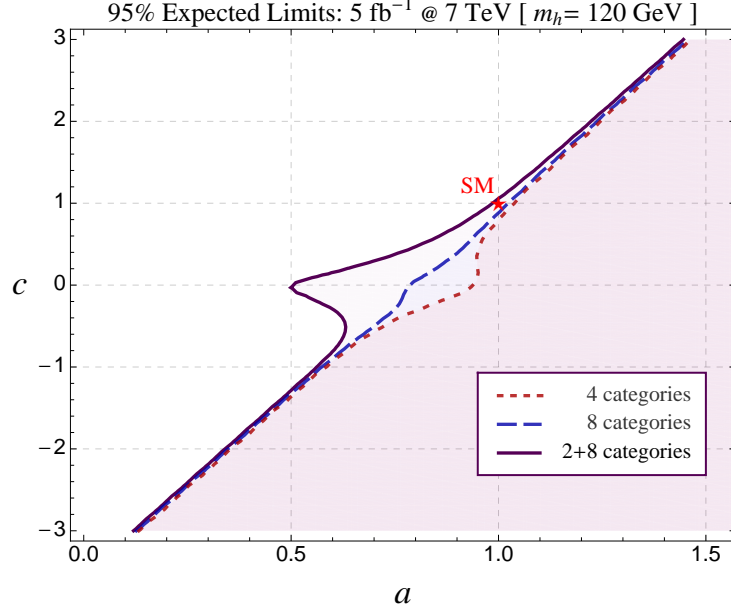


Figure 1: Expected exclusion limits from $\gamma\gamma$ at $\sqrt{s} = 7$ TeV with $L = 5 \text{ fb}^{-1}$ and $m_h = 120$ GeV. Purple solid curve: exclusive analysis with 8+2 categories; Dashed blue curve: inclusive analysis with 8 categories; Dotted red curve: inclusive analysis with 4 categories. The area on the right of each curve is excluded at 95% probability.

vicinity of the SM point, in agreement with the results of Ref. [19].⁴

Interestingly, a further subdivision of the 4 inclusive categories into two sets with respectively large and small $p_T(\gamma\gamma)$ also increases the sensitivity in the fermiophobic region (dashed blue curve). This is because the distribution of the transverse momentum of the $\gamma\gamma$ pair tends to be harder for events produced through VBF and associated production, so that requiring larger values of $p_T(\gamma\gamma)$ increases the relative importance of these production modes compared to gluon fusion. An analysis with 8 categories was performed by CMS in 2011 on 1.66 fb^{-1} of data (a subset of the total 2011 data set) and is reported in Ref. [28]. We find, although the corresponding curve is not shown in Fig. 1, that once the two exclusive categories optimized respectively for VBF and associated production are included in the

⁴We note in passing that for $a = c$ the constraint from the 4-category analysis is stronger than the limit on the signal modifier $\mu^{95\%} = 1.6$ discussed in the previous section. Indeed, it can be shown that a 2D probability with flat prior gives the same limit on the line $a = c$ of a 1D probability with non-flat prior on μ .

analysis, having 8 additional ‘inclusive’ categories instead of 4 does not appreciably improve the sensitivity in the (a, c) plane. In other words, performing an exclusive analysis with 4+2 categories leads to constraints on the couplings a, c quite similar to those obtained with our analysis which makes use of 8+2 categories. This in fact agrees with the naive expectation, considering that the fraction of events produced through VBF and associated production that fall into the inclusive categories is quite small: see Table 1. To summarize, we find that an exclusive analysis of $h \rightarrow \gamma\gamma$ is more powerful than an inclusive one to set limits on the Higgs couplings, especially in regions where the importance of the VBF and associated production modes is enhanced compared to gluon fusion.

A fully exclusive analysis of the $\gamma\gamma$ channel is even more useful once the observation of a signal has been established and it comes to extracting the Higgs couplings. We illustrate this in the following by showing contours of equal probability in the plane (a, c) obtained by injecting a specific signal and assuming $L = 20 \text{ fb}^{-1}$ with $\sqrt{s} = 7 \text{ TeV}$. This should be a reasonable approximation of the data set which will be individually accumulated in 2012 by ATLAS and CMS at $\sqrt{s} = 8 \text{ TeV}$. We have chosen to perform our simulations at 7 TeV (rather than 8) to facilitate comparison with the previous results and to be conservative since it is still not clear what the real performances of the detectors will be with the larger pile-up rate.

Figure 2 illustrates the case of an injected SM signal ($a = 1, c = 1$). The plot on the left shows the 68% probability contours selected by respectively the $jj, 1l$ and (the combination of the eight) inclusive categories. Related results were discussed in Refs. [12, 14, 3, 15, 16, 18], although following different approaches and assumptions than ours. The shape of the various regions can be easily reproduced considering that the yield of the two exclusive categories is dominated respectively by events produced via VBF and associated production, while the inclusive categories are dominated by gluon fusion. Defining the ratio

$$\mu_i = \frac{\sigma_i \times BR(\gamma\gamma)}{[\sigma_i \times BR(\gamma\gamma)]_{SM}} \quad (3.2)$$

as the yield in a given category i in SM units, it thus follows

$$\mu_{jj} \sim \mu_{1l} \sim a^2 \frac{(4.5a - c)^2}{c^2}, \quad \mu_{incl} \sim (c^2 + \zeta a^2) \frac{(4.5a - c)^2}{c^2}, \quad (3.3)$$

where the factor $(4.5a - c)^2$ follows from the branching ratio to $\gamma\gamma$, and ζ parametrizes the small contamination of VBF and VH events in the inclusive categories. Eq. (3.3) reproduces

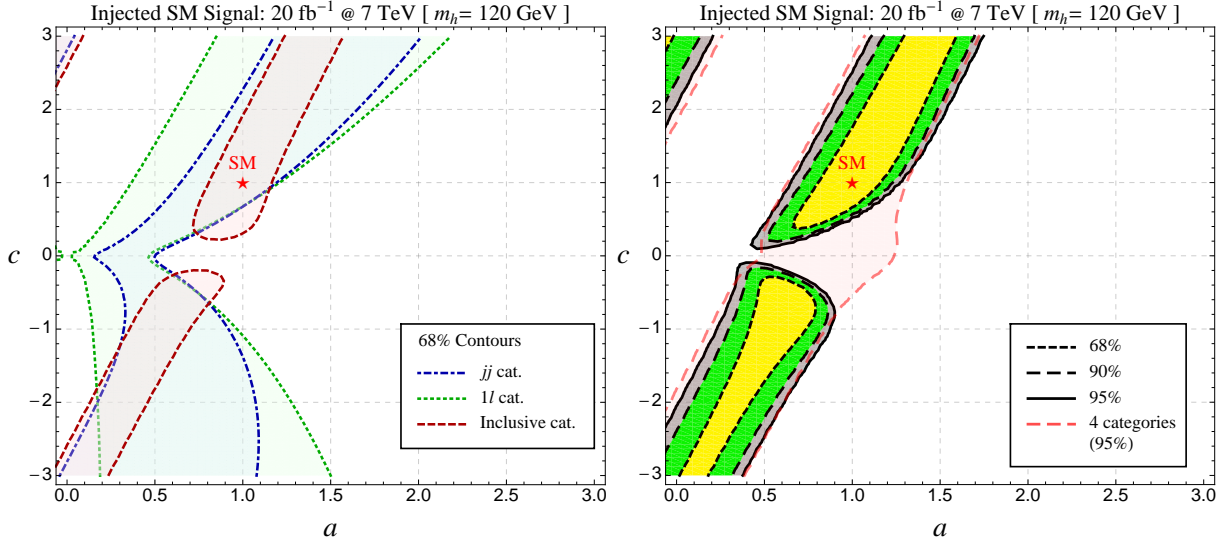


Figure 2: Contours of constant probability for $\gamma\gamma$ in the plane (a, c) obtained by injecting the SM signal ($a = 1, c = 1$). Left plot: 68% contours for the jj , $1l$ and inclusive categories. Right plot: 68%, 90%, 95% contours in the exclusive analysis with 8+2 categories and 95% contour in the inclusive analysis with 4 categories. Both plots are for $\sqrt{s} = 7 \text{ TeV}$ with $L = 20 \text{ fb}^{-1}$ and $m_h = 120 \text{ GeV}$.

to good accuracy the shape of the different regions of Fig. 2. In particular, the non-negligible contribution of VBF and VH events in the inclusive categories with high $p_T(\gamma\gamma)$ (see Table 1) removes the long tail at large a and small c of the area which would be selected by the remaining four inclusive classes with low $p_T(\gamma\gamma)$.⁵ The resulting 68% region selected by the combination of all inclusive categories is that shown in red in the left plot of Fig. 2, which stretches along the line $(4.5a - c) = \text{const.}$ passing through the SM point. We have checked, on the other hand, that the contamination of GGF events in the jj category modifies only marginally the shape of the 68% probability region selected by this category.

For $c \rightarrow 0$ the exclusive jj and $1l$ categories favor values $a < 1$, which ensure a suppression of the production cross section and compensate the strong increase in the branching ratio, as required to reproduce $\mu_{jj,1l} \sim 1$. On the contrary, the region $c \sim 0$ is disfavored for any value of a by the inclusive categories, since their yield is strongly suppressed in the fermiophobic

⁵See for example the upper right plot in Fig. 2 of Ref. [14], where the contribution of VBF and VH events to the inclusive categories was neglected.

limit. As a result, by injecting the SM signal, an exclusive analysis of $h \rightarrow \gamma\gamma$ can exclude the fermiophobic region $c \simeq 0$ with a probability of more than 95%; see the plot on the right in Fig. 2. This is especially true for the benchmark point $(a = 1, c = 0)$, which predicts too many events in the jj and $1l$ categories and too few in the inclusive ones. On the other hand, it is not possible to exclude this point and the region surrounding it by means of a 4-category inclusive analysis; see the dashed red curve in the same plot. Indeed, the total $\gamma\gamma$ yield for $(a, c) \sim (1, 0)$ is approximately that of the SM (see for example the discussion in Ref. [29]), and the overall sensitivity decreases as a consequence of the absence of the clean exclusive categories.

In order to derive an estimate of how the results in Fig. 2 change with the Higgs mass, we have repeated our analysis by varying m_h and assuming that the background yield and the selection efficiencies do not change significantly. This is expected to be a reasonably accurate approximation for $m_h = 120 - 130$ GeV. In this range of masses the variation of the signal yield is driven by the change in the Higgs production cross sections and in the $\gamma\gamma$ branching ratio, with the latter giving the dominant effect. We find that even for $m_h = 130$ GeV the contours of Fig. 2 are only slightly modified. This is because for $(a = 1, c = 1)$ the signal yield, hence the injected one, changes by less than $\sim 15\%$. The larger distortion occurs in the fermiophobic region $c \sim 0$, where the $\gamma\gamma$ branching ratio is enhanced, which is however largely disfavored by combining the inclusive and exclusive categories. We thus conclude that our results hold with good accuracy in the range $m_h = 120 - 130$ GeV.

The exclusive analysis selects two regions with high probability: one includes the SM point, the other corresponds to negative values of c (yellow areas in the right plot of Fig. 2). The presence of a second solution in addition to $(a, c) = (1, 1)$ is a direct consequence of the quadratic dependence of the yields in eq.(3.3) on a, c and the interference of the 1-loop top and W contributions to the $\gamma\gamma$ decay rate: by injecting a given signal (a_0, c_0) , there is a second solution

$$a \simeq a_0 \frac{4.5 a_0 - c_0}{4.5 a_0 + c_0}, \quad c \simeq -c_0 \frac{4.5 a_0 - c_0}{4.5 a_0 + c_0}, \quad (3.4)$$

which gives the same yields μ_{jj} , μ_{1l} and μ_{incl} . For $(a_0, c_0) = (1, 1)$ the second solution corresponds to $(0.64, -0.64)$, which is indeed the position of the second maximum of the 2D probability whose contours are shown in Fig. 2.

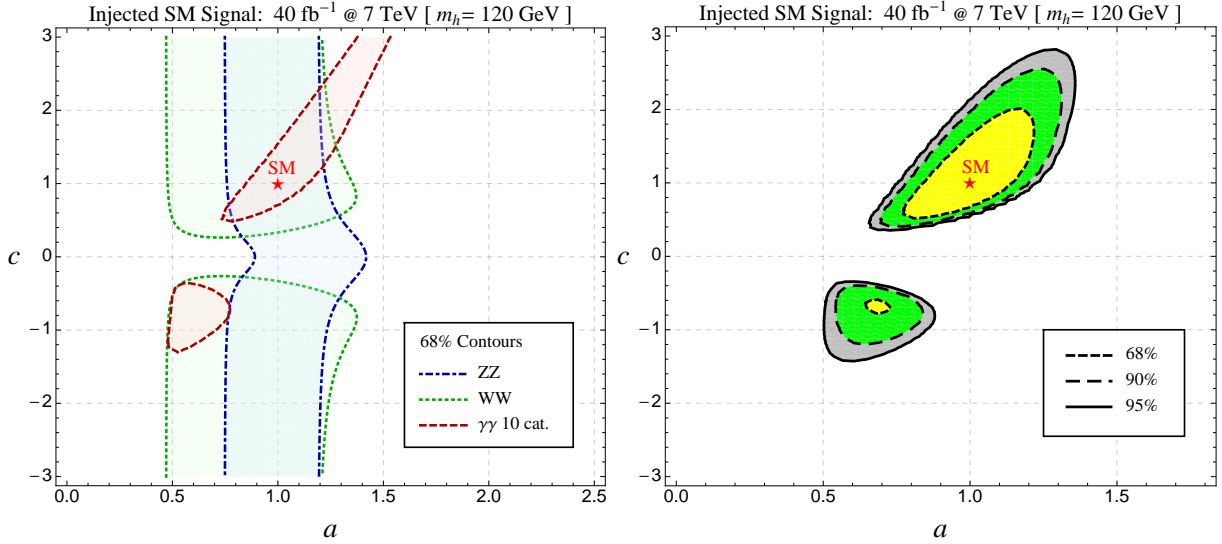


Figure 3: Contours of constant probability in the plane (a, c) for $\gamma\gamma$, ZZ and WW obtained by injecting the SM signal ($a = 1, c = 1$). Left plot: 68% contours for individual $\gamma\gamma$ (10-categories exclusive analysis, red area), $WW \rightarrow l\nu l\nu$ (5-categories exclusive analysis, green area) and $ZZ \rightarrow 4l$ (inclusive analysis, blue area) channels. Right plot: 68%, 90%, 95% contours for their combination. For WW and ZZ the probability function has been constructed by rescaling the number of events reported by CMS respectively in Ref. [30] and Ref. [31]; see text.

The existence of a second degenerate solution in the plane (a, c) was noticed and discussed in Refs. [12, 3, 15, 16, 18]. Breaking such degeneracy will require large integrated luminosity and the combined use of several channels. An extrapolation of the results of the current searches to higher luminosity indicates that the most sensitive channels in this regard are $\gamma\gamma$ and $ZZ \rightarrow 4l$, while others, like WW and $\tau\tau$, are less powerful. Although performing an exclusive analysis for each decay channel will play a crucial role also in this case, a complete resolution of the degeneracy might require considering more refined strategies. This is for example illustrated by Fig. 3, where we show the probability contours obtained at $L = 40 \text{ fb}^{-1}$ (the total amount of integrated luminosity which might be obtained by the end of 2012 by CMS and ATLAS together) from $\gamma\gamma$, $ZZ \rightarrow 4l$ and $WW \rightarrow l\nu l\nu$ (left plot) and their combination (right plot). For the WW channel we have considered the exclusive analysis performed by CMS [30] for $m_h = 120 \text{ GeV}$ (see Ref. [3] for details). In the case of ZZ we have performed a simple cut-and-count analysis by considering the number of signal

and background events expected by CMS in a ± 5 GeV window around $m(4l) = 120$ GeV.⁶ We have constructed the posterior probability by including a 15% systematic error on the signal, while we have neglected the systematic uncertainty on the background since this is expected to be small for a shape-based analysis like $ZZ \rightarrow 4l$ (and similarly $\gamma\gamma$) once sufficient statistics has been accumulated.

As the left plot of Fig. 3 illustrates, the projected sensitivity of the current WW analysis to $L = 40 \text{ fb}^{-1}$ is poor and does not help much to remove the second solution. This is due in large part to the effect of the systematic uncertainties, which are large for WW . It is not clear if this systematic error will be reduced in a future analysis or if it will increase as due to the larger uncertainty on the missing energy measurement which could follow from the higher pile-up rate at 8 TeV. A slightly enhanced sensitivity for WW is expected if the Higgs is heavier than 120 GeV, as the result of the increase in the corresponding branching ratio. The $ZZ \rightarrow 4l$ channel, on the other hand, is much more clean and has a strong impact in disfavoring the second solution. After its inclusion in the fit, the peak of the probability at $a = -c = 0.64$ is ~ 5 times smaller than the peak at $a = c = 1$ (see the right plot of Fig. 3). We have checked that the $\tau\tau$ channel selects a broad region in the (a, c) plane, and it has very little impact on the global fit.⁷ For this reason we have not included it in Fig. 3. In this regard our results do not agree with the early analysis of Ref. [10], which used a much more optimistic estimate of the background and found that $\tau\tau$ was one of the most sensitive channels for $m_h = 120$ GeV.⁸

⁶More specifically we used the right plot of Fig. 2 of Ref. [31] and summed the number of events in five bins around $m(4l) = 120$ GeV. In this way we find $n_s^{SM} = 1.5$, $n_b = 1.7$ respectively for the number of SM signal and background events with $L = 4.7 \text{ fb}^{-1}$. Since the CMS analysis is inclusive, we have rescaled the SM yield in the plane (a, c) by assuming that the cut efficiencies are the same for each of the various production modes. Although this is known to be a very rough approximation, it is the best one can do in absence of more detailed information.

⁷We have made a very crude cut-and-count estimate based on the CMS analysis of Ref. [32]. We find that assuming a 10% systematic uncertainty on the background the precision on the (a, c) plane is very poor. A more refined result would require a detailed analysis which is beyond the scope of this paper.

⁸A similar underestimation of the background for $\tau\tau$ is present also in the analyses of Refs. [11, 12]. See also the discussion and results of Ref. [17] on the expected sensitivity on the Higgs couplings obtained by making use of the actual background estimates and errors reported in the current experimental analyses as compared to earlier Montecarlo studies.

Our results show that by extrapolating the current analyses to 40 fb^{-1} the second solution can be disfavored but not completely eliminated. A complete removal of the degeneracy will require more integrated luminosity or substantial improvements of the present analyses, possibly following from new strategies. The use of ratios of yields in different categories within the same decay channel or different channels, as recently suggested by Ref. [15] as a way to reduce the degeneracy, does not seem to provide a resolution in this case. Its main advantage indeed is that it helps to reduce the systematic uncertainties, which are however already expected to be small for $\gamma\gamma$ and $ZZ \rightarrow 4l$. We find that by setting to zero the systematic error on the signal of both $\gamma\gamma$ and ZZ the contours of Fig. 3 are marginally modified. In particular, the second solution becomes excluded at 68% but the extension of the 90% and 95% probability regions is only slightly reduced. Concentrating on the solution centered at the SM point, the plot of Fig. 3 suggests that with 40 fb^{-1} , if the Higgs is that of the SM, the coupling a can be measured with a precision of $\sim 25\%$, while the uncertainty on c is of the order of 100%. Our estimate for a seems to be in agreement with the recent results of [17], which however reports a significantly smaller uncertainty on c .

We end this section by showing in Fig. 4 the contours of equal probability for an injected signal ($a = 1/\sqrt{2}, c = 0$), for $L = 20 \text{ fb}^{-1}$. We choose this point as representative of a fermiophobic scenario since it is realized in the composite Higgs model MCHM5 [33] and it was already considered in previous works. Notice that although for $m_h = 120 \text{ GeV}$ such choice of couplings is excluded at 95% CL by the current CMS combined results [34], it is still allowed for $123 \text{ GeV} < m_h < 130 \text{ GeV}$.⁹ As expected from Eq. (3.4), in this case there is no degeneracy of solutions. By performing an exclusive analysis, the maximum of the probability is obtained in a small region around $(1/\sqrt{2}, 0)$ where μ_{incl} is small and $\mu_{jj,1l} \sim 5$. The Higgs couplings a, c can be determined in this case with a precision of $\sim 35\%$. On the other hand, an inclusive analysis with 4 categories is dramatically less powerful and selects only a broad region in the plane (red area in the right plot of Fig. 4). We checked that the same qualitative conclusions apply for $m_h = 125 \text{ GeV}$, although the uncertainty on the couplings increases to $\sim 45\%$. On the other hand, for larger Higgs masses the contours of Fig. 4 become quickly broader, and already at $m_h = 130 \text{ GeV}$ the 90% region of the combined

⁹By comparison, the ‘standard’ benchmark point ($a = 1, c = 0$) is excluded at 95% CL in the whole range $110 - 192 \text{ GeV}$ [34].

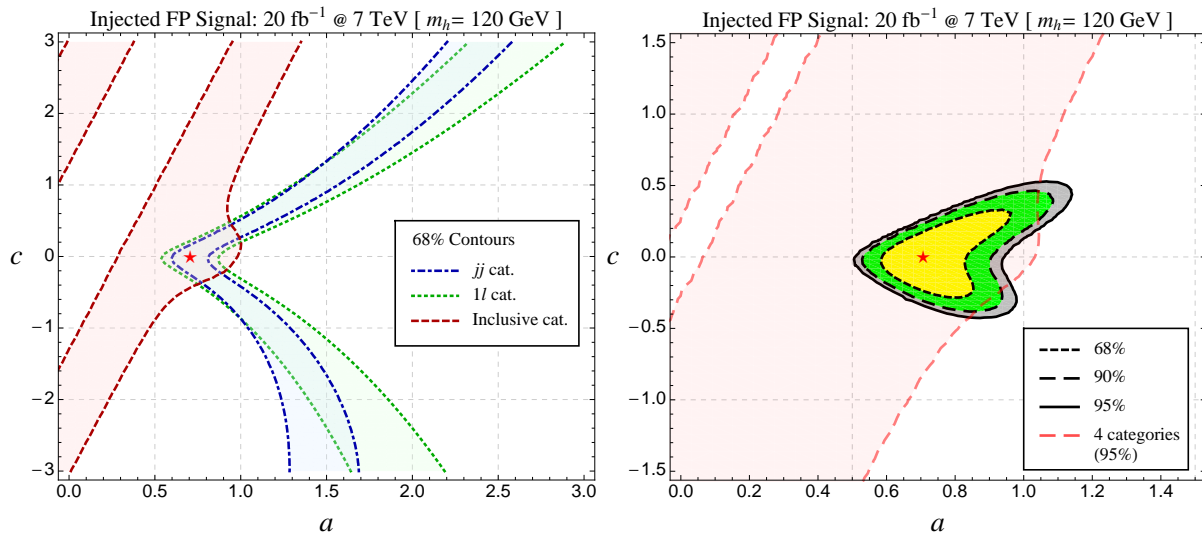


Figure 4: As for Fig. 2 with injected fermiophobic signal ($a = 1/\sqrt{2}$, $c = 0$).

fit forms an open strip in the plane. This is mostly due to the decrease of the injected yield implied by the fast drop of the $\gamma\gamma$ branching ratio at heavier Higgs masses for $c = 0$. We thus conclude that while our results for the fermiophobic case apply reasonably well up to $m_h = 125$ GeV, assessing the precision on the Higgs couplings at larger Higgs masses will require a dedicated analysis.

4 Conclusions

If a Higgs-like scalar is discovered at the LHC in 2012, we will enter a new exciting phase in which the main focus will be on determining its couplings as precisely as possible. This will eventually shed light on the dynamics behind EWSB, confirming or excluding the SM paradigm. It is clear that a correct theoretical interpretation of the experimental results will be crucial in achieving this goal, but much will also depend on the way the analyses are performed and the results presented by the experimental collaborations. This is evident even now, considering the numerous theoretical papers appearing recently [14, 3, 15–18] which try to interpret the results from the LHC searches on the SM Higgs in terms of models of new physics. In fact, a fully correct interpretation is not always possible because the published

experimental papers often do not contain sufficient information. For example, even a crude estimate of the impact of the LHC searches on generic models of new physics requires knowing the cut efficiencies for each of the production modes and each of the event categories. Hopefully, this information will be made public in the future by the experimental collaborations. However, even knowing that, a rigorous determination of the Higgs couplings is possible only by including all the systematic effects and correlations among different categories and different channels. Although a few theoretical groups have taken the challenge seriously (for example the SFitter collaboration [35, 17]), the experimental collaborations themselves seem to be those who can more easily confront this formidable task. The main obstacle in this regard is that performing an analysis necessarily requires *some* assumption about which (class of) models are under scrutiny. This highlights the importance of a consistent theoretical framework that allows one to explore the largest possible landscape of theories with the smallest number of assumptions.

The electroweak chiral Lagrangian introduced in [2, 3] seems to be quite suitable to this aim: it assumes only that there are no new light states in the spectrum beyond a Higgs-like scalar (and thus the Higgs can decay only to pairs of SM particles) and that there is a (at least approximate) custodial symmetry. A further request for the absence of (sizable) Higgs flavor-violating couplings is necessary to comply with the experimental data from FCNC processes. If necessary, the first assumption can be relaxed by introducing in the effective Lagrangian any new light state which will be possibly discovered at the LHC. Under the above hypotheses, the strength of the Higgs interactions is parametrized in terms of a set of parameters which must be determined experimentally. In this enlarged parameter space, the SM corresponds to a point in the vicinity of which the theory stays perturbative up to very high energies. The framework is sufficiently general to describe theories of composite Higgs, supersymmetric theories where the additional scalars are much heavier, and even models where the light scalar is not part of an $SU(2)_L$ doublet or is not related to EWSB like in the case of a dilaton. From a practical point of view, all the Higgs production cross sections and decay fractions can be easily derived from a simple rescaling of SM known expressions. For convenience, we collect in the Appendix the relevant formulas for the simplified case in which only the overall strength of the Higgs coupling to vector bosons, $a = g_{hVV}/g_{hVV}^{SM}$, and to fermions, $c = g_{h\psi\psi}/g_{h\psi\psi}^{SM}$, are free to vary.

In this paper we have made a first attempt to estimate the precision that the LHC can reach on a and c with 2012 data by focusing on the $h \rightarrow \gamma\gamma$ channel, which is the most sensitive for a light Higgs. We have set the Higgs mass to the benchmark value $m_h = 120$ GeV, and discussed how the results change in the range $120 - 130$ GeV. Our first important conclusion is that exclusive analyses are much more powerful than inclusive ones both to put limits on and to precisely measure the Higgs couplings. This is especially true for theories of non-standard Higgses (like fermiophobic models) where the importance of the VBF and associated production is enhanced compared to gluon fusion. A milder though significant improvement is however achieved even for a SM Higgs. It is thus clear that performing analyses in ways that are as exclusive as possible is a crucial strategy for a precise determination of the Higgs couplings. By injecting a SM signal in our simulation, we also found that $\gamma\gamma$ alone selects a second degenerate solution in the plane (a, c) . The degeneracy can be broken only by adding additional channels to the fit. We find that $ZZ \rightarrow 4l$ seems to be the most powerful channel to this aim, since it can lead to a precise determination of the coupling a . Other channels such as WW and $\tau\tau$ turn out to be less precise and their inclusion does not have a strong impact on the fit. Our extrapolation of the current analyses to $L = 40 \text{ fb}^{-1}$ (the total amount of integrated luminosity which might be obtained by the end of 2012 by CMS and ATLAS together) shows that the second solution will be disfavored but is not eliminated. Focusing on the solution centered at the SM point, we estimate that for $m_h = 120$ GeV the precision with which the couplings a and c can be determined at 68% of probability is respectively $\sim 25\%$ and $\sim 100\%$. More refined strategies or a larger amount of luminosity seem to be required in order to completely exclude the second solution and obtain a more precise determination of a and c .

Acknowledgments

We would like to thank Emanuele Di Marco and Simone Gennai for important discussions and suggestions, and Christophe Grojean for discussions and useful comments on the manuscript. The work of R.C. was partly supported by the ERC Advanced Grant No. 267985 *Electroweak Symmetry Breaking, Flavour and Dark Matter: One Solution for Three Mysteries (DaMeSyFla)*.

A Appendix

We collect here the formulas needed to compute the Higgs production cross section and branching fractions in terms of SM values for the case in which the overall strength of the Higgs coupling to vector bosons, $a = g_{hVV}/g_{hVV}^{SM}$, and to fermions, $c = g_{h\psi\psi}/g_{h\psi\psi}^{SM}$, are free to vary. This is a special simplified scenario of the general parametrization of the Higgs couplings introduced in [2, 3]. There are no new production modes nor new decay channels in addition to those present in the SM.

The expression of the four Higgs production cross section is given by a simple rescaling of the SM ones ($V = W, Z$):

$$\begin{aligned}
\sigma(gg \rightarrow h) &= c^2 \sigma(gg \rightarrow h)_{SM} \\
\sigma(qq \rightarrow qqh) &= a^2 \sigma(qq \rightarrow qqh)_{SM} \\
\sigma(q\bar{q} \rightarrow Vh) &= a^2 \sigma(q\bar{q} \rightarrow Vh)_{SM} \\
\sigma(gg, q\bar{q} \rightarrow t\bar{t}h) &= c^2 \sigma(gg, q\bar{q} \rightarrow t\bar{t}h)_{SM}
\end{aligned} \tag{A.5}$$

The decay branching ratios are determined by a simple rescaling of the Higgs partial widths. The formulas for these latter are (f denotes any of the quarks and leptons of the SM):

$$\begin{aligned}
\Gamma(h \rightarrow VV) &= a^2 \Gamma(h \rightarrow VV)_{SM} \\
\Gamma(h \rightarrow f\bar{f}) &= c^2 \Gamma(h \rightarrow f\bar{f})_{SM} \\
\Gamma(h \rightarrow gg) &= c^2 \Gamma(h \rightarrow gg)_{SM} \\
\Gamma(h \rightarrow \gamma\gamma) &= \frac{|c A_f(m_h) + a A_W(m_h)|^2}{|A_f(m_h) + A_W(m_h)|^2} \Gamma(h \rightarrow \gamma\gamma)_{SM} \\
\Gamma(h \rightarrow Z\gamma) &= \frac{|c B_f(m_h) + a B_W(m_h)|^2}{|B_f(m_h) + B_W(m_h)|^2} \Gamma(h \rightarrow Z\gamma)_{SM}
\end{aligned} \tag{A.6}$$

so that $\Gamma_{tot}(h)$ is the sum of the above partial widths and $BR(h \rightarrow X) = \Gamma(h \rightarrow X)/\Gamma_{tot}(h)$.

The functions A and B are given at one loop by

$$A_f(m_h) = -\frac{8}{3} \frac{4m_t^2}{m_h^2} \left[1 + \left(1 - \frac{4m_t^2}{m_h^2} \right) \times f \left(\frac{4m_t^2}{m_h^2} \right) \right], \quad (\text{A.7})$$

$$A_W(m_h) = 2 + 3 \times \frac{4m_W^2}{m_h^2} \left[1 + \left(2 - \frac{4m_W^2}{m_h^2} \right) \times f \left(\frac{4m_W^2}{m_h^2} \right) \right], \quad (\text{A.8})$$

$$B_f(m_h) = -\frac{4 \left(\frac{1}{2} - \frac{4}{3} \sin^2 \theta_W \right)}{\sin \theta_W \cos \theta_W} \left[I_1 \left(\frac{4m_t^2}{m_h^2}, \frac{4m_t^2}{m_Z^2} \right) - I_2 \left(\frac{4m_t^2}{m_h^2}, \frac{4m_t^2}{m_Z^2} \right) \right], \quad (\text{A.9})$$

$$B_W(m_h) = -\frac{\cos \theta_W}{\sin \theta_W} \times \left\{ (12 - 4 \tan^2 \theta_W) \times I_2 \left(\frac{4m_W^2}{m_h^2}, \frac{4m_W^2}{m_Z^2} \right) + \left[\left(1 + \frac{2m_h^2}{4m_W^2} \right) \tan^2 \theta_W - \left(5 + \frac{2m_h^2}{4m_W^2} \right) \right] \times I_1 \left(\frac{4m_W^2}{m_h^2}, \frac{4m_W^2}{m_Z^2} \right) \right\}, \quad (\text{A.10})$$

where

$$I_1(a, b) = \frac{ab}{2(a-b)} + \frac{a^2 b^2}{2(a-b)^2} [f(a) - f(b)] + \frac{a^2 b}{(a-b)^2} [g(a) - g(b)], \quad (\text{A.11})$$

$$I_2(a, b) = -\frac{ab}{2(a-b)} [f(a) - f(b)], \quad (\text{A.12})$$

with

$$f(x) = \begin{cases} [\sin^{-1}(1/\sqrt{x})]^2 & \text{for } x \geq 1 \\ -\frac{1}{4} \left[\log \left(\frac{1+\sqrt{1-x}}{1-\sqrt{1-x}} \right) - i\pi \right]^2 & \text{for } x < 1, \end{cases} \quad (\text{A.13})$$

and

$$g(x) = \begin{cases} \sqrt{x-1} \sin^{-1}(1/\sqrt{x}) & \text{for } x \geq 1 \\ \frac{1}{2} \sqrt{1-x} \left[\log \left(\frac{1+\sqrt{1-x}}{1-\sqrt{1-x}} \right) - i\pi \right]^2 & \text{for } x < 1. \end{cases} \quad (\text{A.14})$$

For a full discussion of these results, and expressions for more general cases where new fields can contribute to the loop functions, see for instance [36].

For simplicity, we quote in Table 3 numerical values of the functions $A_{f,W}$ and $B_{f,W}$ for the mass range of interest. Note that the contribution from gauge bosons in $h \rightarrow Z\gamma$ are on the order of 20 times larger than the contribution from fermions; in practice, modifications to this decay will have a negligible impact on results throughout the space explored in this analysis.

m_h (GeV)	A_f	A_W	B_f	B_W
100	-1.81	7.72	0.635	-10.8
110	-1.82	7.93	0.638	-11.2
120	-1.83	8.19	0.641	-11.7
130	-1.84	8.53	0.644	-12.3
140	-1.85	9.01	0.648	-13.2
150	-1.86	9.76	0.652	-14.7
160	-1.87	12.40	0.657	-20.0

Table 3: Numerical values for rescaling factors in loop-mediated processes $h \rightarrow \gamma\gamma$ and $h \rightarrow Z\gamma$.

References

- [1] D. B. Kaplan and H. Georgi, Phys. Lett. B **136** (1984) 183. S. Dimopoulos and J. Preskill, Nucl. Phys. B **199**, 206 (1982). T. Banks, Nucl. Phys. B **243**, 125 (1984). D. B. Kaplan, H. Georgi and S. Dimopoulos, Phys. Lett. B **136**, 187 (1984). H. Georgi, D. B. Kaplan and P. Galison, Phys. Lett. B **143**, 152 (1984). H. Georgi and D. B. Kaplan, Phys. Lett. B **145**, 216 (1984). M. J. Dugan, H. Georgi and D. B. Kaplan, Nucl. Phys. B **254**, 299 (1985).
- [2] R. Contino, C. Grojean, M. Moretti, F. Piccinini and R. Rattazzi, JHEP **1005** (2010) 089 [arXiv:1002.1011 [hep-ph]].
- [3] A. Azatov, R. Contino and J. Galloway, arXiv:1202.3415 [hep-ph].
- [4] J. F. Donoghue, C. Ramirez and G. Valencia, Phys. Rev. D **39** (1989) 1947; J. F. Donoghue and C. Ramirez, Phys. Lett. B **234** (1990) 361; J. Bagger, V. D. Barger, K. -m. Cheung, J. F. Gunion, T. Han, G. A. Ladinsky, R. Rosenfeld and C. -P. Yuan, Phys. Rev. D **52** (1995) 3878 [hep-ph/9504426].
- [5] E. Halyo, Mod. Phys. Lett. A **8** (1993) 275. W. D. Goldberger, B. Grinstein and W. Skiba, Phys. Rev. Lett. **100** (2008) 111802 [arXiv:0708.1463 [hep-ph]]; L. Vecchi, Phys. Rev. D **82** (2010) 076009 [arXiv:1002.1721 [hep-ph]]; B. A. Campbell, J. Ellis and K. A. Olive, arXiv:1111.4495 [hep-ph].

- [6] G. F. Giudice, C. Grojean, A. Pomarol and R. Rattazzi, JHEP **0706** (2007) 045 [arXiv:hep-ph/0703164].
- [7] D. Zeppenfeld, R. Kinnunen, A. Nikitenko and E. Richter-Was, Phys. Rev. D **62** (2000) 013009 [hep-ph/0002036].
- [8] J. Conway *et al.* [Precision Higgs Working Group of Snowmass 2001 Collaboration], eConf C **010630** (2001) P1WG2 [hep-ph/0203206].
- [9] A. Belyaev and L. Reina, JHEP **0208** (2002) 041 [hep-ph/0205270].
- [10] M. Duhrssen, “Prospects for the measurement of Higgs boson coupling parameters in the mass range from 110 – 190 GeV/ c^2 ”, ATL-PHYS-2003-030.
- [11] M. Duhrssen, S. Heinemeyer, H. Logan, D. Rainwater, G. Weiglein and D. Zeppenfeld, Phys. Rev. D **70** (2004) 113009 [arXiv:hep-ph/0406323].
- [12] R. Lafaye, T. Plehn, M. Rauch, D. Zerwas and M. Duhrssen, JHEP **0908** (2009) 009 [arXiv:0904.3866 [hep-ph]].
- [13] S. Bock, R. Lafaye, T. Plehn, M. Rauch, D. Zerwas and P. M. Zerwas, Phys. Lett. B **694** (2010) 44 [arXiv:1007.2645 [hep-ph]].
- [14] D. Carmi, A. Falkowski, E. Kuflik and T. Volansky, arXiv:1202.3144 [hep-ph].
- [15] J. R. Espinosa, C. Grojean, M. Muhlleitner and M. Trott, arXiv:1202.3697 [hep-ph].
- [16] P. P. Giardino, K. Kannike, M. Raidal and A. Strumia, arXiv:1203.4254 [hep-ph].
- [17] M. Rauch, arXiv:1203.6826 [hep-ph]; M. Klute, R. Lafaye, T. Plehn, M. Rauch, D. Zerwas, M. Duhrssen, in preparation.
- [18] J. Ellis and T. You, arXiv:1204.0464 [hep-ph].
- [19] S. Chatrchyan *et al.* [CMS Collaboration], “Search for the standard model Higgs boson decaying into two photons in pp collisions at $\sqrt{s}=7$ TeV,” arXiv:1202.1487 [hep-ex] (accepted by PLB).

- [20] CMS Collaboration, “Search for the fermiophobic model Higgs boson decaying into two photons,” CMS-PAS HIG-12-002.
- [21] J. Alwall, P. Demin, S. de Visscher, R. Frederix, M. Herquet, F. Maltoni, T. Plehn and D. L. Rainwater *et al.*, JHEP **0709**, 028 (2007) [arXiv:0706.2334 [hep-ph]].
- [22] T. Sjöstrand, S. Mrenna, and P.Z. Skands, PYTHIA 6.4 Physics and Manual, JHEP **0605**, 026 (2006) doi:10.1088/1126-6708/2006/05/026.
- [23] S. Alioli, P. Nason, C. Oleari and E. Re, JHEP **0904**, 002 (2009) [arXiv:0812.0578 [hep-ph]].
- [24] P. Nason and C. Oleari, JHEP **1002**, 037 (2010) [arXiv:0911.5299 [hep-ph]].
- [25] CMS Collaboration, “Search for a Higgs boson decaying into two photons in the CMS detector”, CMS-PAS HIG-11-030.
- [26] G. D’Agostini, “Bayesian reasoning in data analysis: A critical introduction,” New Jersey, USA: World Scientific (2003) 329 p
- [27] ATLAS and CMS Collaborations and LHC Higgs Combination Group, *Procedure for the LHC Higgs boson search combination in Summer 2011*, CMS-NOTE-2011/005; ATL-PHYS-PUB-2011-11 (2011).
- [28] CMS Collaboration, “Search for a Higgs boson decaying into two photons in the CMS detector”, CMS-PAS HIG-11-021.
- [29] E. Gabrielli, B. Mele and M. Raidal, arXiv:1202.1796 [hep-ph].
- [30] S. Chatrchyan *et al.* [CMS Collaboration], “Search for the standard model Higgs boson decaying to a W pair in the fully leptonic final state in pp collisions at $\sqrt{s} = 7$ TeV,” arXiv:1202.1489 [hep-ex] (accepted by PLB).
- [31] S. Chatrchyan *et al.* [CMS Collaboration], “Search for the standard model Higgs boson in the decay channel H to ZZ to 4 leptons in pp collisions at $\sqrt{s} = 7$ TeV,” arXiv:1202.1997 [hep-ex] (accepted by PRL).

- [32] S. Chatrchyan *et al.* [CMS Collaboration], “Search for neutral Higgs bosons decaying to tau pairs in pp collisions at $\sqrt{s}=7$ TeV,” arXiv:1202.4083 [hep-ex] (accepted by PLB).
- [33] R. Contino, L. Da Rold and A. Pomarol, Phys. Rev. D **75** (2007) 055014 [arXiv:hep-ph/0612048].
- [34] CMS Collaboration, “Combined results of searches for a Higgs boson in the context of the standard model and beyond-standard models”, CMS-PAS HIG-12-008.
- [35] R. Lafaye, T. Plehn and D. Zerwas, hep-ph/0404282.
- [36] J. F. Gunion, H. E. Haber, G. L. Kane and S. Dawson, “The Higgs Hunter’s Guide,” Front. Phys. **80**, 1 (2000).